Numerical Analysis of Compound Semiconductor RF Devices

V. Palankovski, S. Wagner, and S. Selberherr

Institute for Microelectronics, TU Vienna, Gusshausstrasse 27-29, A-1040 Vienna, Austria
E-mail: Palankovski@iue.tuwien.ac.at

Abstract

An overview of heterostructure RF device simulation for industrial application based on III-V compound semiconductors has been given in [1]. Here, we present the most recent achievements in numerical simulation for industrial heterostructure devices, together with relevant industrial applications (GaAs, InP, and SiGe HBTs).

INTRODUCTION

To cope with explosive development costs and strong competition in the semiconductor industry today, Technology Computer-Aided Design (TCAD) methodologies are extensively used in development and production. Several questions during device fabrication, such as performance optimization and process control, can be addressed by simulation. The choice of a given simulation tool or a combination of tools depends to a large extent on the complexity of the particular task, on the desired accuracy of the problem solution, and on the available human, computer, and time resources.

Optimization of geometry, doping, materials, and material compositions targets high output power, high breakdown voltage, high speed (high f_T and f_{max}), low leakage, low noise, and low power consumption. This is a challenging task that can be significantly supported by device simulation. While DC simulation is sufficient for optimization of breakdown voltages, turn-on voltages, or leakage currents, AC simulation is required for speed, noise, and power issues.

There are several challenges which are specific for modeling and simulation of heterostructure devices [2]. The characterization of the physical properties of III-V and SiGe compounds is required for wide ranges of material compositions, temperatures, doping concentrations, etc. The model parameters must be verified against several independent HEMT and HBT technologies to obtain a concise set used for all simulations.

For example, the database for novel materials, such as the GaN or the GaSb systems, which have entered the III-V world with impressive device results, is still relatively poor. Modeling of stress-induced changes of the physical properties of strained material layers and consideration of piezoelectrical effects is a subject of ongoing research [2]. Heterointerface modeling is a key issue for devices which include abrupt junctions. Thermionic emission, field emission, and tunneling effects critically determine the current transport, especially in double heterojunction bipolar transistors (DHBTs).

Advanced device simulation allows a precise physics-based extraction of small-signal parameters [2]. Measured bias-dependent S-parameters serve as a valuable source of information when compared at different bias points to simulated S-parameters from a device simulator. By simulating in the frequency domain, important small-signal figures of merit, such as the cut-off frequency f_T and the maximum oscillation frequency f_{max} can be efficiently extracted [3]. On the other hand, non-linear periodic steady-state analysis can be performed in the time domain to obtain large-signal figure-of-merit parameters, such as distortion, power, frequency, noise, etc. [4] as well in the context of coupled device and circuit simulation.

HETEROSTRUCTURE DEVICE SIMULATORS

The continuously increasing computational power of computer systems allows the use of TCAD tools on a very large scale. Several commercial device simulators (such as [5]-[10]) company-developed simulators (such as [11]-[13]), and university-developed simulators (like [14]-[19]) have been successfully employed for device engineering applications. These simulators differ considerably in dimensionality (one, quasi-two, two, quasi-three, or three), in choice of carrier transport model (drift-diffusion, energy-transport, or Monte Carlo statistical solution of the Boltzmann transport equation), and in the capability of including electrothermal effects. The drift-diffusion transport model [20] is by now the most popular model used for device simulation. With down-scaling of the feature sizes, non-local effects become more pronounced and must be accounted for by applying an energy-transport model or a hydrodynamic transport model [21]. During the last two decades, Monte Carlo methods for solving the Boltzmann transport equation have been developed [22] and applied for device simulation [23, 24]. However, reduction of computational resources is still an issue, and therefore Monte Carlo device simulation is still not feasible for industrial application on daily basis. An approach to preserve accuracy at lower computational cost is to calibrate lower order transport parameters to Monte Carlo simulation data.

SELECTED RESULTS OF INDUSTRIALLY RELEVANT DEVICES

Two-dimensional device simulation proved to be valuable for understanding the underlying device physics [25] and for improving the device reliability [26]. Bias-dependent S-parameters hold the full small-signal RF information about the device behavior and allow process control beyond the information about the DC quantities.

As an example, by means of two-dimensional device AC simulation with MINIMOS-NT [19], we extracted the S-parameters for a one-finger InGaP/GaAs HBT with emitter area of 3×30 μm^2 [27]. The combined Smith-polar chart in Fig. 1 shows good agreement between simulated and measured S-parameters at V_{CE} = 3 V and current density J_C = 2 kA/cm^2 for the frequency range between 50 MHz and 10 GHz.

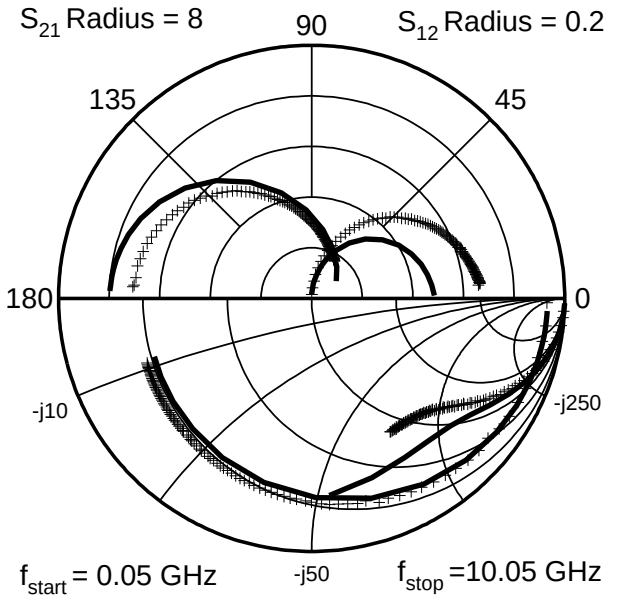

Figure 1: Simulated (–) and measured (+) S-parameters in a combined Smith-polar chart from 50 MHz to 10 GHz at V_{CE} = 3 V and J_C = 2 kA/cm^2.

In addition, we set up a mixed-mode circuit to compare large-signal measurement data in the small-signal range. Fig. 2 gives simulated AC collector current i_C versus AC input power P_{IN} in good agreement with experimental data. Fig. 3 shows a comparison between measured and simulated AC output power P_{OUT} versus AC input power P_{IN}. An almost perfect match of the curves is achieved in the small-signal area of the figure. A further increase of the input power causes harmonics in the device, which can not be obtained by the linear small-signal mode. Several methods which account for harmonic generation in the device, e.g. the harmonic balance method, have been evaluated in [28]. A software platform that integrates harmonic balance RF simulation technologies into an analogue/mixed signal design flow framework is offered by Agilent [12].

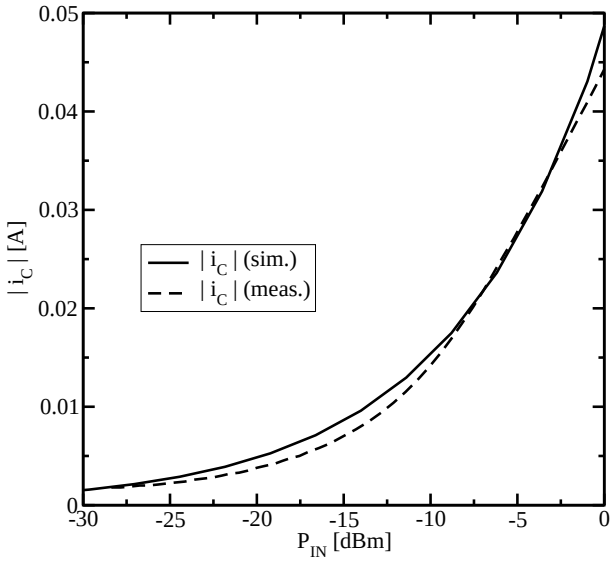

Figure 2: Comparison of simulated and measured AC collector current i_C vs. AC input power P_{IN}.

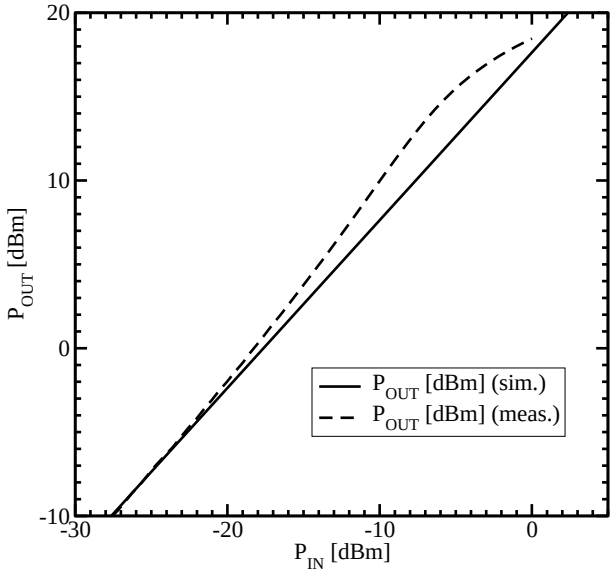

Figure 3: Comparison of simulated and measured AC output power P_{OUT} vs. AC input power P_{IN}.

In another example we investigated a nominally 1×8 μm^2 InP/InGaAs/InGaAsP/InP DHBT self-aligned device structure with a typical cut-off frequency of about 130 GHz and breakdown voltage of $BV_{CE0} = 5.5$ V. Tunneling mechanisms which dominate electron transport between the device must be properly accounted for in the interface models. In addition high-field/high-energy electron transport in InGaAs and InP (respectively the quarternary InGaAsP), which determines both the steady-state and small-signal device behavior, has been carefully modeled. Other important issues which have been solved in the course of our work are proper modeling of the energy bandgaps and bandgap align-

ments between InGaAs and InP, and the bandgap narrowing effect at high doping concentrations, especially in p^+ InGaAs. Fig. 4 shows a comparison of intrinsic S-parameters at $V_{CE} = 1.1\,V$ and $V_{BE} = 0.91\,V$ in a frequency range between 250 MHz and 120 GHz.

A detailed discussion and comparison of various InP single HBTs and DHBTs, such as InP/InGaAs/InGaAsP/InP and InP/GaAsSb/InP HBTs, is given in [2].

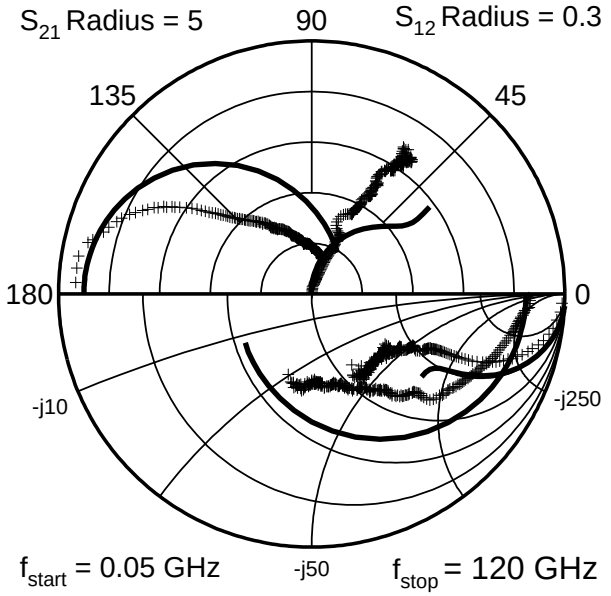

Figure 4: Simulated (–) and measured (+) intrinsic S-parameters in a combined Smith-polar chart from 50 MHz to 120 GHz at V_{CE} = 1.1 V and V_{CE} = 0.91 V

MINIMOS-NT was further applied to industrial $12 \times 0.4\ \mu m^2$ SiGe HBTs. All important physical effects, such as surface recombination, impact ionization (II) generation, and self-heating (SH), are properly modeled and accounted for in the simulation in order to get good agreement with measured forward and output (Fig. 5) characteristics using one concise set of models and parameters [29]. It must be noted that simulation without including self-heating effects cannot reproduce the experimental data, especially at high power levels. A closer look at the increasing collector current I_C at high collector-to-emitter voltages V_{CE} and constant base current I_B, stepped by 0.4 μA from 0.1 μA to 1.7 μA, reveals the interplay between self-heating and impact ionization generation. While impact ionization generation leads to a strong increase of I_C, self-heating decreases it. In fact, both I_C and I_B increase due to self-heating at a given bias condition. As the change is higher for I_B, in order to maintain I_B at the same level, V_{BE} and, therefore, I_C decrease. A proper DC calibration is an important prerequisite for AC simulation [3]. The consideration of anisotropic electron mobility in the strained SiGe base is demonstrated in Fig. 6. In addition, results obtained by a commercial device simulator (DESSIS [8]), using default models and parameters, are included for comparison.

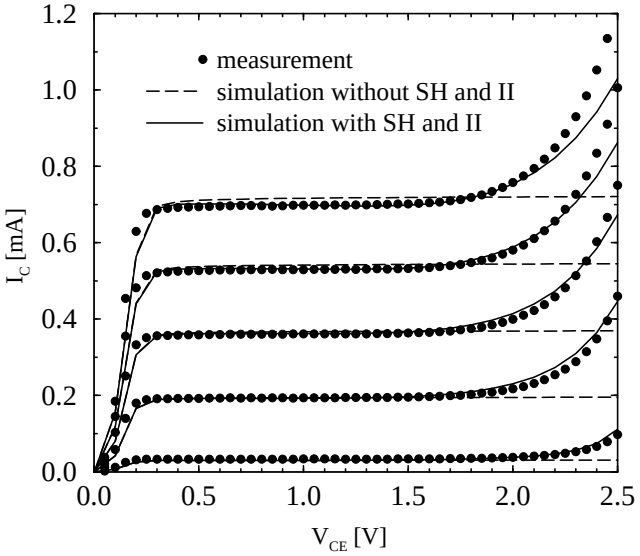

Figure 5: Simulated output characteristics with and without self-heating (SH) and impact ionization (II) and comparison to measurements. I_B is stepped by 0.4 μA from 0.1 μA to 1.7 μA.

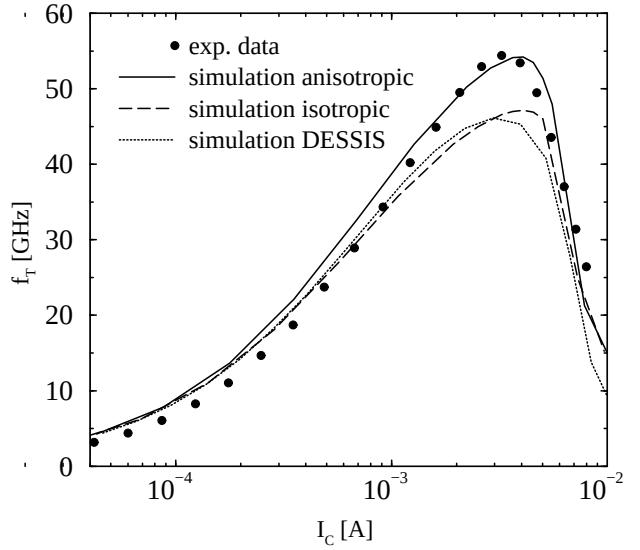

Figure 6: Simulated (anisotropic with solid line, isotropic with dashed line, DESSIS with dotted line) and measured (with circles) current gain cut-off frequency f_T versus collector current I_C at V_{CE} = 1 V.

Once calibrated, the simulator can be further applied to devices from different technologies and different vendors. For example, Fig. 7 shows a forward Gummel plot of an six-finger $20 \times 0.25\ \mu m^2$ SiGe HBT. The third harmonic intercept voltage parameter V_{IP3} is considered to give a good indication of the device linearity. As suggested in [30], V_{IP3} can be obtained from DC characteristics. The results derived by this approach prove that it is applicable also to SiGe HBTs.

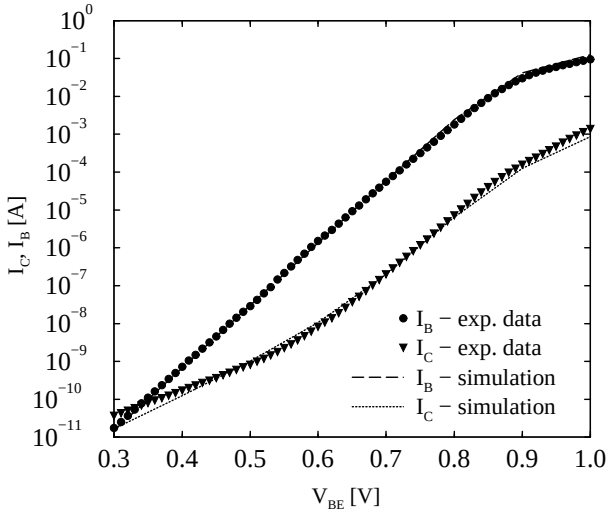

Figure 7: Forward Gummel plots at V_{CB} = 0 V: Comparison between measurement data and simulation at room temperature.

ACKNOWLEDGMENTS

This work is supported by the Austrian Science Fund (FWF), Project P14483-MAT, by Christian-Doppler-Laboratory for TCAD in Microelectronics, Austria, by austriamicrosystems AG, Unterpremstätten, Austria, by Infineon Technologies AG, Munich, Germany, and by the Fraunhofer Institute of Applied Solid-State Physics, Freiburg, Germany.

REFERENCES

[1] V. Palankovski, R. Quay, and S. Selberherr, "Industrial Application of Heterostructure Device Simulation," in *GaAs IC Symp.Tech.Dig.*, pp. 117–120, 2000, (invited).

[2] V. Palankovski and R. Quay, *Analysis and Simulation of Heterostructure Devices*, Wien, New York: Springer, 2003.

[3] S. Wagner, V. Palankovski, T. Grasser, G. Röhrer, and S. Selberherr, "A Direct Extraction Feature for Scattering Parameters of SiGe-HBTs," in *Intl. SiGe Technology and Device Meeting*, (Nagoya), pp. 83–84, 2003.

[4] Y. Hu and K. Mayaram, "Periodic Steady-State Analysis for Coupled Device and Circuit Simulation", in *Simulation of Semiconductor Processes and Devices*, (Seattle), pp. 90–94, 2000.

[5] APSYS, http://www.crosslight.com/downloads/

[6] ATLAS/Blaze, http://www.silvaco.com/products/vwf/

[7] BIPOLE3, http://www.bipsim.com/mainframe.html

[8] DESSIS and DIOS, http://www.ise.com/products/

[9] G-PISCES-2B, http://www.gateway-modeling.com/

[10] MEDICI, http://www.synopsys.com/products/avmrg/

[11] E. Buturla, P. Cottrell, B. Grossman, and K. Salsburg, "Finite-Element Analysis of Semiconductor Devices: The FIELDAY Program," http://www.research.ibm.com/journal/rd/441/buturla.pdf

[12] *A Comprehensive Guide to Harmonic Balance Simulation in RFDE*, Agilent Technologies, 2003. http://eesof.tm.agilent.com/docs/

[13] NEMO, http://www.cfdrc.com/nemo/

[14] PISCES-ET, http://www-tcad.stanford.edu/tcad.html

[15] FLOODS/FLOOPS, http://www.tec.ufl.edu/flooxs/

[16] J. Geßner, F. Schwierz, H. Mau, D. Nuernbergk, M. Roßberg, and D. Schipanski, "Simulation of the Frequency Limits of SiGe HBTs," in *Proc. Intl.Conf. on Modeling and Simulation of Microsystems*, (San Juan), pp. 407–410, 1999.

[17] DEVICE, http://www.uv.ruhr-uni-bochum.de/

[18] nextnano3, http://www.webplexity.de/nextnano3.php

[19] MINIMOS-NT Device and Circuit Simulator, http://www.iue.tuwien.ac.at/software/minimos-nt.

[20] S. Selberherr, *Analysis and Simulation of Semiconductor Devices*. Wien, New York: Springer, 1984.

[21] T. Grasser, T. Tang, H. Kosina, and S. Selberherr, "A Review of Hydrodynamic and Energy-Transport Models for Semiconductor Device Simulation," *Proc.IEEE*, vol. 91, no. 2, pp. 251–274, 2003.

[22] C. Jungemann and B. Meinerzhagen, *Hierarchical Device Simulation: The Monte-Carlo Perspective.* Wien, New York: Springer, 2003.

[23] H. Kosina, M. Nedjalkov, and S. Selberherr, "Theory of the Monte Carlo Method for Semiconductor Device Simulation" *IEEE Trans. Electron Devices*, vol. 47, no. 10, pp. 1898–1908, 2000.

[24] M. Fischetti and S. Laux, "Performance Degradation of Small Silicon Devices Caused by Long-Range Coulomb Interactions," *Appl.Phys.Let.*, vol. 76, no. 16, pp. 2277–2279, 2000.

[25] V. Palankovski, R. Schultheis, and S. Selberherr, "Simulation of Power Heterojunction Bipolar Transistors on Gallium Arsenide," *IEEE Trans.Electron Devices*, vol. 48, no. 6, pp. 1264–1269, 2001.

[26] V. Palankovski, S. Selberherr, R. Quay, and R. Schultheis, "Analysis of HBT Degradation After Electrothermal Stress," in *Simulation of Semiconductor Processes and Devices*, (Seattle), pp. 245–248, 2000.

[27] S. Wagner, V. Palankovski, T. Grasser, R. Schultheis, S. Selberherr. "Small-Signal Analysis and Direct S-Parameter Extraction" in *Intl.Symp. on Electron Devices for Microwave and Optoelectronic Applications EDMO*, (Manchester), pp. 50–55, 2002.

[28] K.S. Kundert, "Introduction to RF Simulation and Its Application", *IEEE J.Solid-State Circuits*, vol. 34, no. 9, pp. 1298-1319, 1999.

[29] V. Palankovski, G. Röhrer, T. Grasser, S. Smirnov, H. Kosina, and S. Selberherr, "Rigorous Modeling Approach to Numerical Simulation of SiGe-HBTs," in *Intl. SiGe Technology and Device Meeting*, (Nagoya), pp. 97–98, 2003.

[30] P.H. Woerlee, M.J. Knitel, R. van Langevelde, D.B.M. Klaassen, L.F. Tiemeijer, A.J. Scholten, A.T.A Zegers-van Duijnhoven, "RF-CMOS Performance Trends" *IEEE Trans.Electron Devices*, vol. 48, no. 8, pp. 1776–1782, 2001.